Polymeric-Based Epoxy Cured with a Polyaminoamide as an Anticorrosive Coating for Aluminum 2024-T3 Surface: Experimental Studies Supported by Computational Modeling

O. Dagdag[1] · R. Hsissou[1] · A. Berisha[2] · H. Erramli[3] · O. Hamed[4] · S. Jodeh[4] · A. El Harfi[1]

Abstract

The present research focused on a coating formulation for aluminum surface 2024-T3 to protect it from corrosion. The formulation consisted of a polymeric epoxy resin-coated bisphenol A diglycidyl ether (DGEBA) cured with a polymeric polyaminoamide. The coated aluminum 2024-T3 was tested in a harsh environment of electrolyte solution (3 wt% NaCl solution) to simulate the harsh marine environment. The coated sample was evaluated by Electrochemical Impedance Spectroscopy (EIS). Under these conditions, a very high impedance (Z) value was obtained; even after exposure for a period longer than 4392 h, the performance was still acceptable. Surface morphological study of metallic specimens before and after exposures to the simulated marine environment (3 wt% NaCl) was carried out using scanning electron microscopy (SEM). The results indicate that the DGEBA-polyaminoamide (DGEBAAA) performed as an excellent barrier for Al surface. The results were combined by several modeling approaches involving molecular dynamics simulation (MD), Monte Carlo methods (MC), and the electronic density functional theory (DFT) computations to explore the adhesion forces between the DGEBAAA and the aluminum surface. The computational MD, MC, and DFT studies were executed in aqueous media. Computational results further evidenced the stronger DGEBA-aminoamide adhesion onto the aluminum 2024-T3 even in a wet environment.

Keywords DGEBA-polyaminoamide · Coating · AA2024-T3 · EIS · DFT · MD and MC simulation

1 Introduction

Organic-based materials are widely used as anticorrosive coating for aluminum structures especially those used in aeronautics and automobiles [1–3]. Organic coatings are

✉ O. Dagdag
omar.dagdag@uit.ac.ma

✉ O. Hamed
ohamed@najah.edu

[1] Laboratory of Agroresources, Polymers and Process Engineering, Department of Chemistry, Faculty of Science, Ibn Tofail University, BP 133, 14000 Kenitra, Morocco

[2] Department of Chemistry, Faculty of Natural and Mathematics Science, University of Pristina, 10000 Pristina, Kosovo

[3] Laboratory of Materials, Electrochemistry and Environment, Department of Chemistry, Faculty of Sciences, Ibn Tofail University, Kenitra, Morocco

[4] Department of Chemistry, An-Najah National University, P. O. Box 7, Nablus, Palestine

known to strongly bond with metal surface thus preventing interfacing between the corrosion reagent and the metal surface. In general, the performance of the anticorrosion agent is strongly dependent on the physicochemical properties of the interface [4]. To this end, several researchers have attempted to explore the adhesion mechanism at the metal–coating interface by examining the physicochemical characteristics and the adhesion performance [5].

It has been generally agreed that metal surface directly affects the properties of a metal–polymer interface [6]. Nonetheless, providing a direct view on the interface considering molecular/atomic-level interactions has remained as an awkward situation. Many methods have been proposed to probe transitions in metal–polymer interfacial state, and there are still some serious weak points associated with experimental investigations, for they are mostly deteriorative to the interface. As a result, the literature lacks a comprehensive framework for demonstrating chemical interfacial interaction between metal substrate and polymer coating layers from a molecular/atomic perspective. Computational modeling and simulation

techniques are powerful tools for tracking interfacial interactions at a molecular/atomic level, and provide a detailed picture of interfacial evolutions [7, 8].

Molecular dynamics (MD) and Monte Carlo (MC) simulation can give detailed information on the atomic level about interactional developments and time evolution of a given complex system [9]. The quantum chemical studies are considered a powerful tool to determine the most stable, conformable structure of the molecule and its electronic properties. Anticorrosive coating mechanism can be determined by analyzing the active sites of coating using DFT (Density Functional Theory) methods.

In the present study, in the first part, a polymeric-based epoxy (DGEBA) cured with a polyaminoamide was prepared and applied on the aluminum 2024-T3 surface. The epoxy resin (DGEBA) has a unique structure that makes it ideal for this purpose. The electrophilic caps and the hydrophobic backbone add two useful properties to the coating: water repellency and strong binding to the metal surface. The anticorrosive properties of the cured DGEBA were monitored by the electrochemical impedance spectroscopy (EIS). The coating surface was monitored using a SEM. In the second part, the interfacial adhesion of epoxy resin coating materials onto aluminum substrates was studied from computational perspectives. Computational investigations using MD and MC simulations were carried out in wet environments. Besides the MD and MC simulations, the electronic structural properties of DGEBA-polyaminoamide responsible for its adsorption behavior were assessed via ab initio quantum mechanics method applying density functional theory (DFT).

2 Experimental

2.1 Materials and methods

The epoxy resin (DGEBA) and hardener (Polyaminoamide) used in this work were procured from MAPAERO-Aerospace Coatings. They were used as received. The structures of these materials are shown in Fig. 1.

2.1.1 Preparation process of aluminum AA2024-T3 substrate

The three aluminum AA2024-T3 substrates used in this study were provided by Casablanca Aeronautics Group Figeac (Morocco). Details of their elemental compositions are summarized Table 1. The aluminum AA2024-T3 samples were degreased with methyl ethyl ketone (MEK) and dried in air for 1 h before coatings.

2.1.2 DGEBA-polyaminoamide coating

The epoxy resin was prepared by mixing at 2:1 ratio by weight of polyaminoamide hardener and epoxy resin (DGEBA). The mixture of the two components was stirred at a speed of 1000 rpm for 20 min. The produced formulation was subjected to the application of air spray technique on the aluminum alloy substrate. Coated substrates were then dried and cured at 60 °C for 1 h. The thickness of coatings was measured to be in the range of 15–25 μm.

2.1.3 Curing process

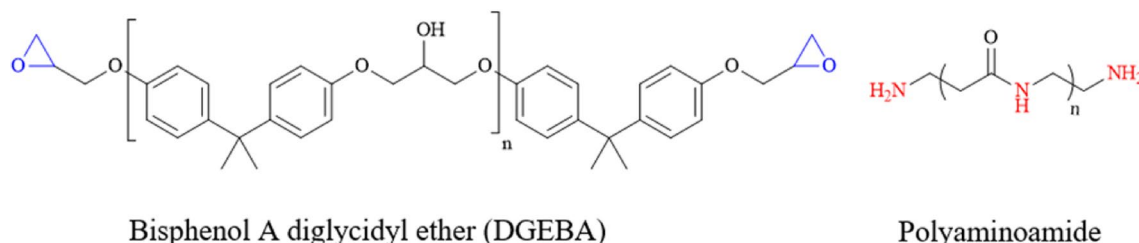The coated plates were placed in an oven at 60 °C for 1 h to complete the curing.

Fig. 1 Molecular structures of the epoxy resin and polyaminoamide used in this study

Table 1 Elementary chemical compositions in weight percent of the studied aluminum 2024-T3

Element	Zn	Mg	Cu	Cr	Mn	Si	Fe	Ti	Al
2024-T3	0.25	1.2–1.8	3.8–4.9	0.10	0.3–0.9	0.50	0.50	0.15	Balance

During the curing process, the epoxy resin and the curing agent polyaminoamide react to form a 3D thermoset polymer with multicoordination sites of hydroxyl and amino groups [10, 11]. The possible chemical structure of the curing product of DGEBA-polyaminoamide is shown in Fig. 2.

2.2 Characterization

2.2.1 Fourier Transform Infrared (FT-IR)

The interactions between DGEBA-polyaminoamide-steel were evaluated using FTIR-attenuated total reflection technique model Bruker, applying a resolution of 4 cm^{-1} and an acquisition of 100 scans.

2.2.2 EIS Measurements

EIS evaluation of the coated aluminum samples was carried in 3 wt% NaCl solution at 298 K using Potentiostat BioLogic SP-200 instrument. Three-electrode cell system was used for electrochemical measurement. The electrode cell system consists of aluminum 2024-T3 as a working electrode (WE), Pt as a counter electrode (CE), and calomel electrode (SCE) as a reference electrode (RE). The EIS measurements were carried out at an open-circuit potential (OCP) with frequency ranging from 100 kHz to 0.01 Hz, and an AC amplitude of 10 mV at OCP. The EIS results were analyzed using EC-Lab V10.32 software fitting procedure.

The anticorrosion performance of the coated substrates was evaluated in an accelerated environment using a salt spray chamber according to ASTM B117 standard.

2.2.3 Surface Characterization

The surface morphologies of the coated aluminum samples before and after exposure to accelerated environment for 4362 h were recorded using scanning electron microscopy (SEM, S3000H, Hitachi) with an accelerated voltage of 20 keV.

2.3 Computational Details

2.3.1 Quantum Chemical Calculations

The relation between the molecular structures and the anti-corrosive performance of the coating was studied by quantum chemical calculation for the polymer repeat unit DGE-BAAA in the neutral form. This was chosen to model the corrosion-protective film formation capacity of the organic coating material-based DGEBAAA on aluminum substrates. Figure 3 displays the chemical structure for monomer DGEBAAA.

The potential energy of polymer repeat unit DGEBAAA was minimized by means of electronic-structure calculations. Such an electronic-scale study was particularly conducted to elucidate fundamental electronic/atomic views regarding the adhesion features of coating molecule above aluminum layers.

The molecular properties of the repeat unit DGE-BAAA were calculated using Material Studio software 6.0 equipped with the DMol3 module. Spin-polarized DFT calculations were performed using the Generalized Gradient Approximation (GGA) and a
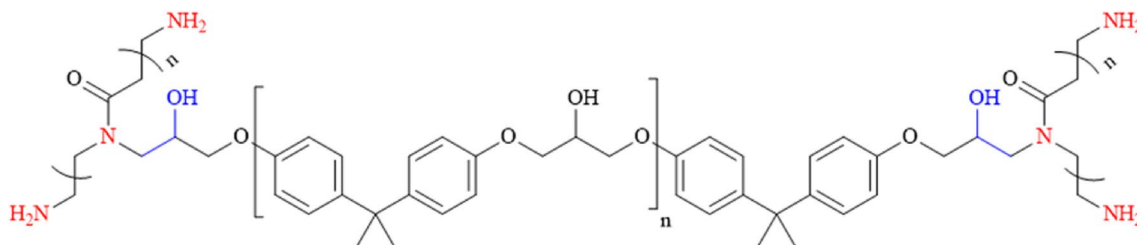

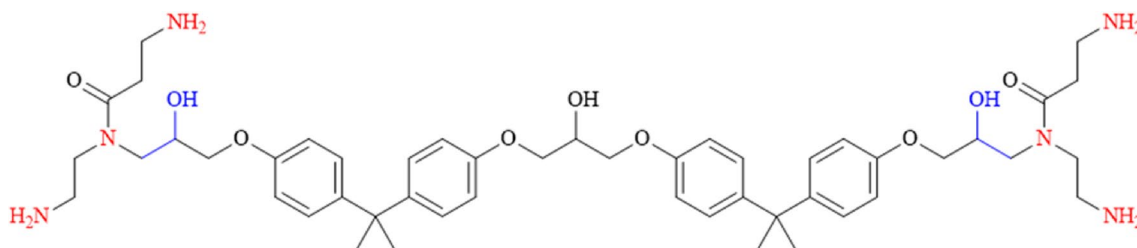**Fig. 2** The polymer's structure of DGEBA-polyaminoamide

Fig. 3 The chemical structure of monomer DGEBAAA

Perdew–Burke–Ernzerhof (PBE) functional. The calculations were based on a triple-numerical polarization (TNP) basis set. The convergence tolerances of energy, maximum force, and displacement were 1.0×10^{-6} Ha, 0.002 Ha/Å, and 0.005 Å, respectively. The Grimme DFT-D method is employed to account for the van der Waals (vdW) interactions [12]. The solvent was described using a Conductor-like Screening Model (COSMO) [13].

2.3.2 Molecular Dynamic (MD) Simulation

MD simulation studies of DGEBAAA adsorptive behavior of aluminum were conducted in an aqueous NaCl media. MD simulation studies were performed using Materials studio 6.0 software [14–17] which has been used to build DGEBAAA molecules and aluminum (111) surface using the sketching tools provided in Materials Visualizer.

The adsorption of the monomer DGEBAAA molecule on the Al (111) side was simulated using the Forcite module. The simulation (both MC and MD) was performed using a surface of Al (111), with cell dimensions $a = b = 63$ Å, containing a 45 Å vacuum layer along the C axis. After fixing the positions of all aluminums bottom layer atoms secured and leaving the top two layers without any constraints, the vacuum layer was filled with one DGEBAAA molecule, 600 molecules of water (H_2O), and 100 Na^+: 100 Cl^- ions. After the filling was completed, the structure of the entire system was optimized, and then the system was subjected to molecular dynamics simulation using a constant temperature (at 298 K), constant volume (NVT) ensemble coupled to Berendsen thermostat (0.1 ps decay constant) [18]. The process parameters are set as follows: COMPASS II (Condensed-phase Optimized Molecular Potentials for Atomistic Simulation Studies) [19] is used as the force field. The simulation was performed using a 1 fs time step with a total simulation time of 500 ps.

2.3.3 Monte Carlo (MC) Simulation

The Metropolis Monte Carlo (MC) method was used to determine the adsorption configurations (using COMPASS II, force field) of the interaction between the monomer DGEBAAA and the surface of the substrate Al (111).

The MC modeling was performed using Adsorption Locator module of Materials Studio software (version 6), and the convergence levels for energy, force, and displacement terms were set to be 1×10^{-4} kcal/mol, 5×10^{-3} kcal/mol/Å, and 5×10^{-5} Å, respectively.

3 Results and Discussion

3.1 FT-IR Analysis

The FT-IR spectrum of DGEBA-polyaminoamide on the aluminum after coating is shown in Fig. 4. The characteristic absorption peaks shown in the spectrum are as follows: a strong broad peak appears in the 3600–3200 cm^{-1} band which could be related to O–H-stretching vibrations. The absorption bands at around 2985 and 2835 cm^{-1} correspond to the stretching vibrations of C–H. The absorption peaks at 1605, 1487, and 1455 cm^{-1} reveal the presence of the aromatic ring. The bands within the range of 1000–1400 cm^{-1} are attributed to the stretching vibrations of C–O and C–N, respectively.

3.2 EIS Measurements

The Nyquist plots of DGEBA-polyaminoamide organic coating materials for aluminum surface 2024-T3 in 3 wt% NaCl solution for different times of exposures are shown in Fig. 5a.

For further investigations, electrical equivalent circuit was used to fit and simulate two-time constant impedance data as shown in Fig. 5b. The electrochemical circuit was used to obtain R_{ct}, R_{coat}, Q_{coat}, and Q_{dl} values from the Nyquist plots.

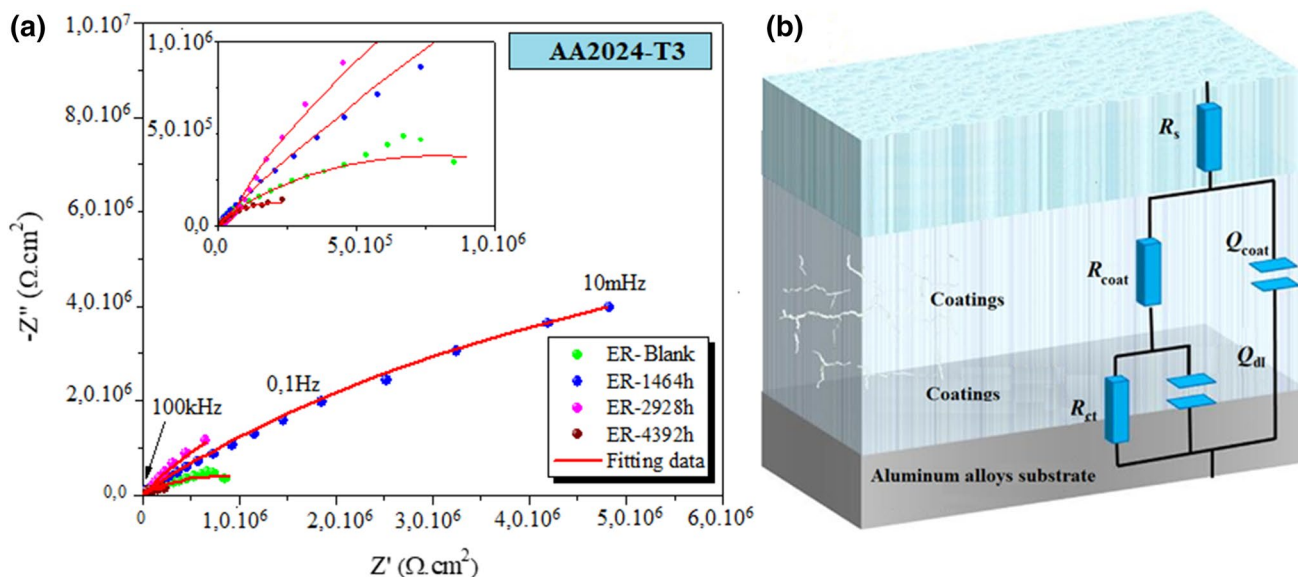**Fig. 4** FT-IR spectrum of DGEBA-polyaminoamide on aluminum surface
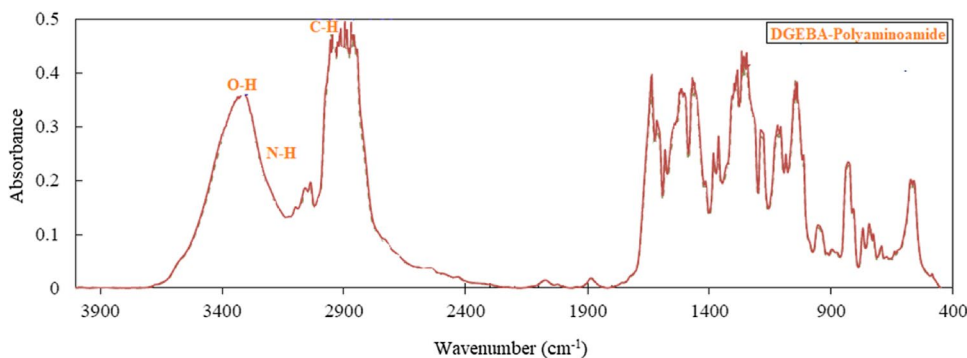
Fig. 5 Nyquist plots obtained for the DGEBA-polyaminoamide organic coating materials for aluminum surface 2024-T3 in 3 wt% NaCl solution for different times of exposures

In Fig. 5b, the values of R_s, R_{coat}, R_{ct}, Q_{coat}, and Q_{dl} are representing solution resistance, coating resistance, charge-transfer resistance, coating capacitance, and double-layer capacitance, respectively. The coating capacitance values (Q_{coat} and Q_{dl}) were calculated using Eq. (1) [20]:

$$Z_{CPE} = \frac{1}{Q(j\omega)^{\alpha'}}, \qquad (1)$$

where Q represents the capacity, CPE is the nonideal capacity, $j = \sqrt{-1}$, ω is the angular frequency (rad/s), and α is a CPE exponent associated with the surface heterogeneity. The electrochemical parameters are given in Table 2.

At the beginning, during the first 2 h of immersion in 3 wt% NaCl solution, the total resistance ($R_t = R_{coat} + R_{ct}$) of the DGEBA polyaminoamide coating was about 2.2 MΩ cm^2. The total resistance (R_t) value of the DGEBA-polyaminoamide coating increased to about 5.7 MΩ cm^2 at 1464 h of immersion. These results confirm that the coating has excellent physical barrier properties

and restricted the electrolyte penetration to the coating/ aluminum interface. Later, it dropped to 0.70 MΩ cm^2 at 4392 h of immersion. The decrease in the total resistance value with times of exposures could be related to the diffusion of the electrolyte into the coating, and thus the physical barrier properties of the film is reduced (after 1464–4392 h). After the longer period of exposure to electrolyte, the coating started to deteriorate, leading to the electrolyte penetration and reaching the coating/ aluminum interface which caused the destruction of the adhesion bonds.

The results of the R_{coat} and R_{ct} values for DGEBA-polyaminoamide coating at different times of exposure are summarized in Table 2. From the impedance diagrams, the coating resistance (R_{coat}) and the charge-transfer resistance (R_{ct}), were used to evaluate the protection performance of the coatings. The R_{coat} (HF) and R_{ct} (LF) values were determined considering the time constants at high frequency and low frequency, respectively.

Table 2 The values of electrochemical parameters of DGEBAAA coating for AA2024-T3 at different times of exposures and 2 h of immersion in 3 wt% NaCl solution

Sample	R_s (Ω cm^2)	CPE$_{coat}$		R_{coa} (kΩ cm^2)	CPE$_{dl}$		R_{ct} (kΩ cm^2)	χ^2
		Q_{coat} (μF/cm^2)	n_{coat}		Q_{dl} (μF/cm^2)	n_{dl}		
0002 h	42.5 (±4.5)	1.45 (±0.8)	0.76	0.70 (±0.08)	0.14 (±0.01)	0.74	1.51 (±0.02)	0.32
DGEBAAA 1464 h	28.9 (±2.8)	0.33 (±0.5)	0.92	0.76 (±0.05)	0.15 (±0.01)	0.73	4.93 (±0.03)	0.19
2928 h	56.1 (±3.4)	0.28 (±0.2)	0.63	0.65 (±0.04)	0.61 (±0.01)	0.72	1.35 (±0.02)	0.06
4392 h	19.4 (±1.2)	0.21 (±0.1)	0.67	0.61 (±0.02)	0.87 (±0.01)	0.72	0.14 (±0.01)	0.07

The R_{coat} indicates the ease with which the penetration of NaCl solution occurs into the DGEBA-polyaminoamide coating [21].

During the first 2 h–1464 h of exposure, the R_{coat} and R_{ct} values of DGEBA-polyaminoamide were much higher. Exposure period longer than 1464 h caused the R_{coat} and R_{ct} values of the coating started to drop. After 2928 h of exposure, the R_{coat} and R_{ct} values of the coating continued to decrease.

As mentioned above the observed results could be attributed to the penetration of the coating surface by water and electrolytes. Extending the exposure to long period of time, caused the water and corrosive electrolytes to reach the coating/metal interface causing an oxidation on metal surface and leading to a corrosion on the aluminum surface.

The analysis of the capacitance of organic coating materials made it possible to evaluate the adsorption of water for at different times of exposure, since the adsorption of water modifies the dielectric constant of the organic coating materials, even if it is present in a very small quantity.

During the first 2 h of immersion in 3 wt% NaCl solution, Q_{coat} of DGEBA-polyaminoamide coating was about 1.4 µF/cm^2. After 1464 h of exposure, the Q_{coat} of coating dropped to a stable, which could be attributed to the delamination of coating materials and filling the micropores causing defects in coating layer [22].

However, the Q_{dl} value which is related to the distribution of ionic charge at metal/coating interface [23] was about 0.14 µF/cm^2 during the first 2 h of immersion in 3 wt% NaCl solution. The value of Q_{dl} was increased by extending the immersion time due to the expansion of the active sites [24].

3.3 Surface Morphology

The surface morphology of DGEBA-polyaminoamide coating on aluminum surface 2024-T3 was monitored by SEM.

The obtained images before and after exposures for 4392 h to salt spray test chamber are shown in Fig. 6. As shown in Fig. 6, the DGEBA-polyaminoamide coating shows a homogeneous surface before exposure. After exposure, the surfaces with the micropores in DGEBA-polyaminoamide coating were developed.

3.4 Theoretical Studies

Computational DFT and calculations of MD and MC simulations were performed over varied experiments to gain basic electronic-/atomic-scale insights into the affinity of DGEBAAA molecules to adsorb and form corrosion-resistant films onto aluminum surfaces.

3.4.1 Global Quantum Chemical Descriptors

DFT study was conducted in both gas as well as in aqueous solution using COSMO model. The energy values of the frontier molecular orbitals (E_{LUMO} and E_{HOMO}) were obtained from the optimized structure, and the rest of DFT parameters were calculated using following equations as described in previous studies [25, 26]:

$$\Delta E = E_{LUMO} - E_{HOMO}, \tag{2}$$

$$I = -E_{HOMO}; A = -E_{LUMO}, \tag{3}$$

$$\chi = \frac{I + A}{2}; \mu = -\chi, \tag{4}$$

$$\eta = \frac{I - A}{2} \quad \text{and} \quad \sigma = \frac{1}{\eta} = -\frac{2}{E_{HOMO} - E_{LUMO}}, \tag{5}$$

$$\omega = \frac{\mu^2}{2\eta} \quad \text{and} \quad \varepsilon = \frac{1}{\omega}, \tag{6}$$
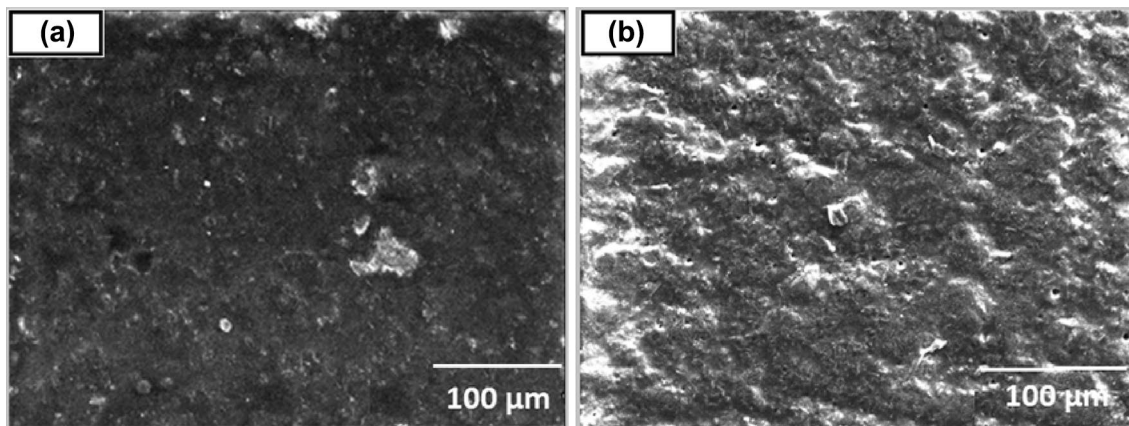

Fig. 6 MEB surface images of the DGEBA-polyaminoamide coating applied on AA 2024-T3 samples **a** before and **b** after 4392-h exposure
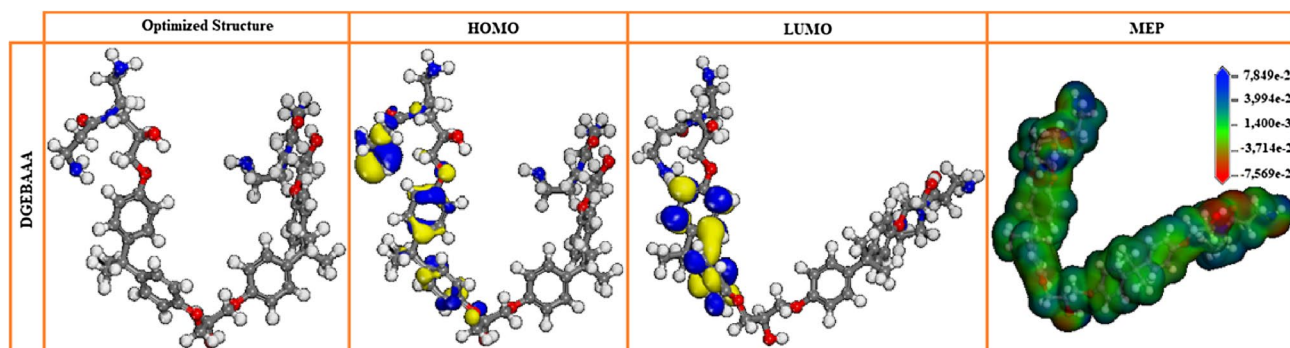
Fig. 7 Optimized structure, HOMO, LUMO orbitals, and MEP of the monomer DGEBAAA using DMol3 module

Table 3 Different quantum chemical parameters in eV of monomer DGEBAAA

	E_{HOMO}	E_{LUMO}	ΔE_{gap}	I	A	χ	μ	η	σ	ω	ε
Values	−5.089	−1.289	3.8	5.089	1.289	3.189	−3.189	1.9	0.52	2.67	0.37

where I, A, ΔE, χ, μ, η, σ, ω, and ε denote the ionization energy, electron affinity, energy band gap, global electronegativity, global chemical potential, global hardness, global softness electrophilicity, and global nucleophilicity, respectively.

The optimized structure and frontier molecule orbital density distributions, namely, HOMO and LUMO orbitals of the monomer DGEBAAA, are shown in Fig. 7. Figure 7 shows the optimized monomer DGEBAAA molecule and the plots of HOMO as well as LUMO. It is obvious from graphical HOMO and LUMO results that the HOMO is distributed on both aromatic rings and it is the nearest to O, N atoms, while LUMO is presented only on one aromatic rings moiety. As a result, the observed preferred flat alignment of the adsorbed coating onto aluminum is rationalized by the presence of these donor–acceptor interactions [27]. The related quantum chemical parameters are summarized in Table 3. The higher value of E_{HOMO}, the lower value of E_{LUMO}, and the lower value of ΔE are consistent with high metal-DGEBAAA interactions and therefore ensure high protection. More importantly, the energy gap plays a significant role in the comparison between coating molecules, especially when they have similar molecular structures. The molecule associated with lower value of ΔE is also related with high softness, lower hardness, and high chemical reactivity thereby with high corrosion-protective ability [14, 15]. The molecular electrostatic potential (MEP) map gives information about the electronic density distributions within the molecule. The MEP map of the studied monomer DGEBAAA is given in Fig. 7. Blue and red regions in the MEP map refer to the areas of positive and negative potentials and compatible with the electron-affluent and electron-poor areas, respectively; it is clear that the negatively charged regions correspond to nitrogen in C–N and oxygen atoms
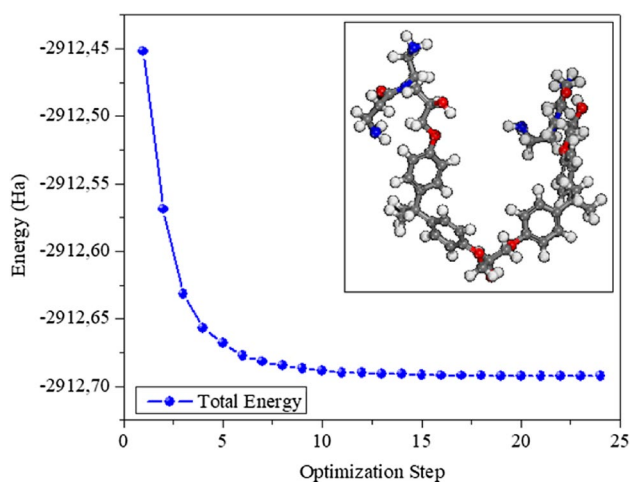

Fig. 8 Optimization energy of monomer DGEBAAA in the neutral forms

in C–O. These electron-rich regions would be the preferred sites for adsorption onto aluminums surface [28, 29]. The lowest electron density is located on the carbon atoms.

3.5 MD Simulation

3.5.1 Energy Optimization a Simulation System

The adsorption of the polymer DGEBAAA onto the aluminum surface was optimized using a MD simulation to understand the interactions between the DGEBAAA repeat unit of the coating and the aluminum surface. MD simulation can reasonably predict the most favorable configuration at the Al (110)/DGEBAAA + 600H$_2$O + 100Na$^+$ and 100Cl$^-$ ions system interface. Figure 8 shows the energy

curve of the polymer repeat unit of the DGEBAAA coating in its optimized neutral and isolated forms before being placed onto the surface of the aluminum substrate using the DMol3.

3.5.2 Analyzing RDFs of the Simulation System

The radial distribution function (RDF) (or paired correlation function), $g(r)$, can be obtained after performing the MD analysis. The RDF is used as a useful method to estimate the length of the link. The peak occurred from 1 Å up to 3.5 Å, which is an indication of the length of small bonds, and is correlated with chemisorption. On the other hand, physical interactions are associated with peaks greater than 3.5 Å.

After analyzing the MD simulation trajectory of Al (111)-DGEBAAA system at 298 K, the RDFs of Al (111)—O (DGEBAAA molecule), Al (111)—N

(DGEBAAA molecule), and Al (111)—C (DGEBAAA molecule) were obtained. All the $g(r)$ curves are depicted in Fig. 8. As shown in Fig. 9, the peak of the $g(r)$ (Al (111)—O) curve appears at about 2.5 Å in the system of Al (111)-DGEBAAA, and it is much bigger than the predicted covalent bond length of Al—O (1.96 Å) [30]. This indicates that the nonbonding interactions exist between the atoms of O (DGEBAAA repeat unit) and Al (111). Similar conclusions can be drawn when analyzing the interactions between the atoms of N (DGEBAA repeat unit) and Al (111).

3.5.3 Ascertaining the Equilibrium of the Simulation System

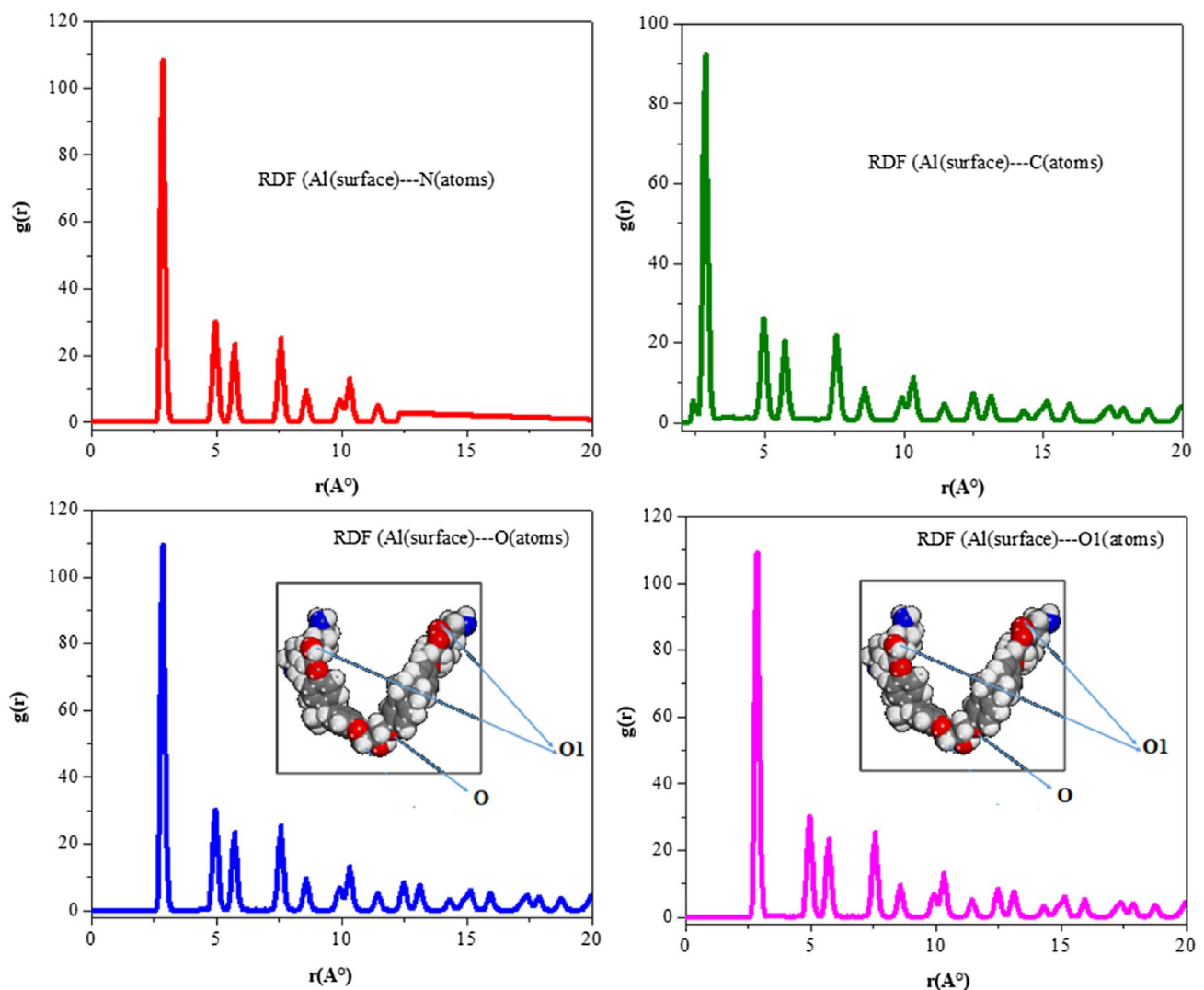To realize an atomic-level comprehension regarding the coating ability of DGEBAAA repeat unit, MD simulations

Fig. 9 Radial distribution functions of the monomer DGEBAAA on Al (111) surface

of coating adsorption onto Al (111) surface representative of aluminum were carried out.

Before analyzing the MD simulation results, the equilibration of simulated cells were assessed utilizing thermodynamic properties including temperature and potential energy.

Figure 10 depicts the time evolution of these properties within the last 500 ps of NVT MD simulations for the repeat unit of DGEBAAA-Al (111). It can be seen from this figure that the temperature and the potential energy

remained unchanged, and their fluctuations throughout the 500 ps MD simulation time are slight, which can serve as an indication for equilibrium attainment.

To further investigate the interaction between the DGEBAAA repeat unit and the Al (111) surface, the MD simulations was performed.

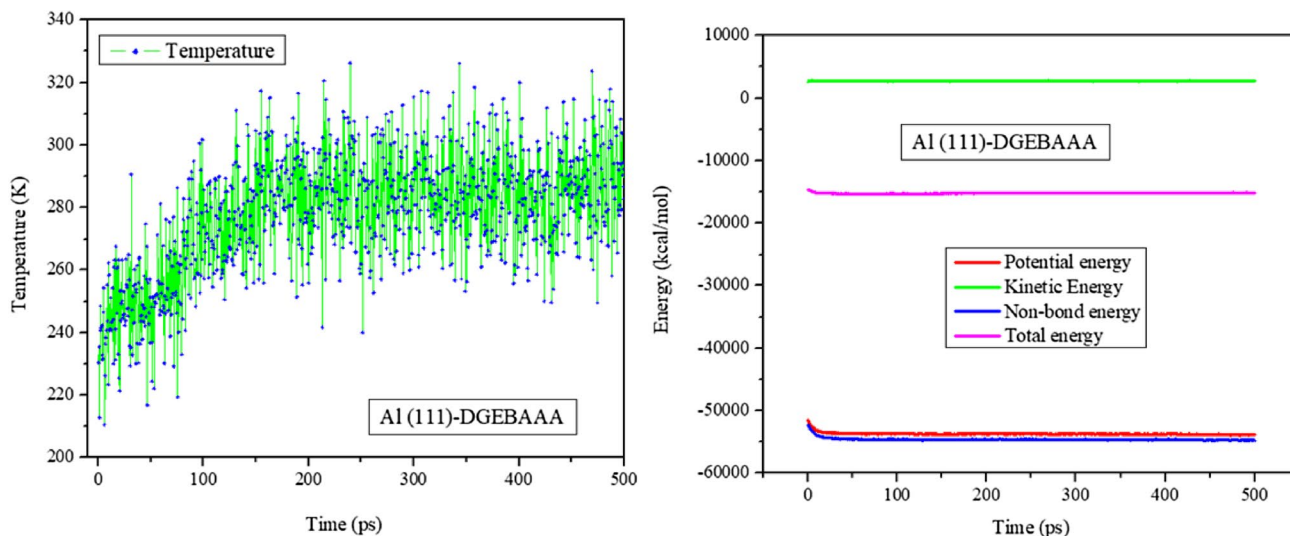Figure 11 shows the side and the on-top views of the equilibrium adsorption configuration of the investigated

Fig. 10 Temperature and energy equilibrium curves of the monomer DGEBAAA molecules adsorbed on the Al (111) surface in NaCl solution
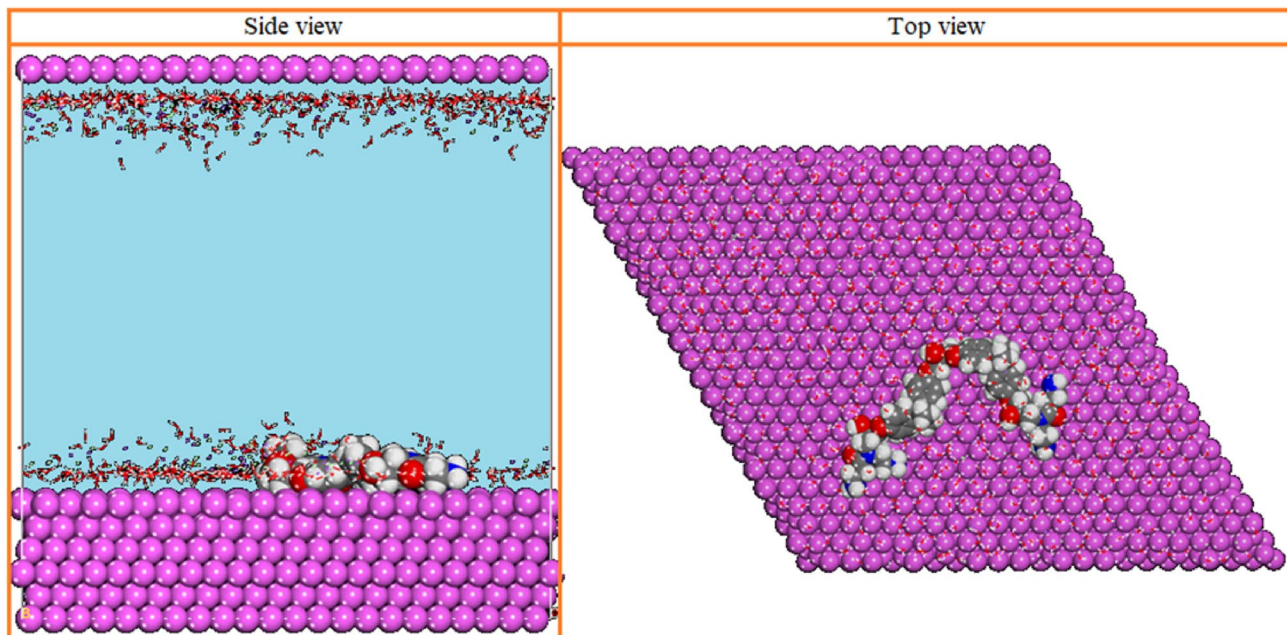

Fig. 11 Top and side views of the most stable low-energy configurations for the adsorption of the monomer DGEBAAA on Al (111) surface obtained using Molecular dynamic simulations

DGEBAAA repeat unit coatings on Al (111) surface $600H_2O + 100Na^+$ and $100Cl^-$ ions system molecules.

Inspection of the top and the side views of the obtained simulation cells indicates that the repeat unit of the DGEBAAA coating on Al (111) surface under humid situations. It can be seen that DGEBAAA repeat unit is localized in the vicinity of aluminum surface by adopting a flat orientation relative to surface.

3.6 Monte Carlo Simulation

3.6.1 Adsorption Energy Distribution of the Simulation System

The adsorption of DGEABAAA repeat unit was evaluated using the Monte Carlo simulation on Al (111) surface at a fixed temperature. The adsorption energy distributions for systems Al (111)-DGEBAAA in NaCl medium obtained by adsorption locator module are shown in Fig. 12.

As observed in Fig. 12, the adsorption energy of DGEBAAA repeat unit reaches -252.06 kcal/mol. This indicates that there is a strong adsorptive interaction of this molecule with the metal surface.

The total energy, average total energy, Van der Waals energy, under study, for Al (111)-DGEBAAA in NaCl solution are calculated by optimizing the whole systems, and the results are shown in Fig. 13.

The energy profile for the equilibrium adsorption configuration as the optimization progresses with steps for Al (111)-DGEBAAA + $600H_2O$ + $100Na^+$ and $100Cl^-$ ions system is shown in Fig. 13. The energy profile clearly shows the optimization of the energy parameters associated with
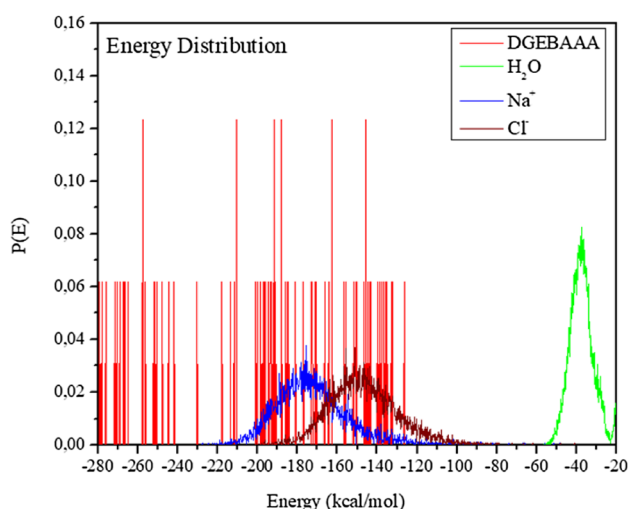

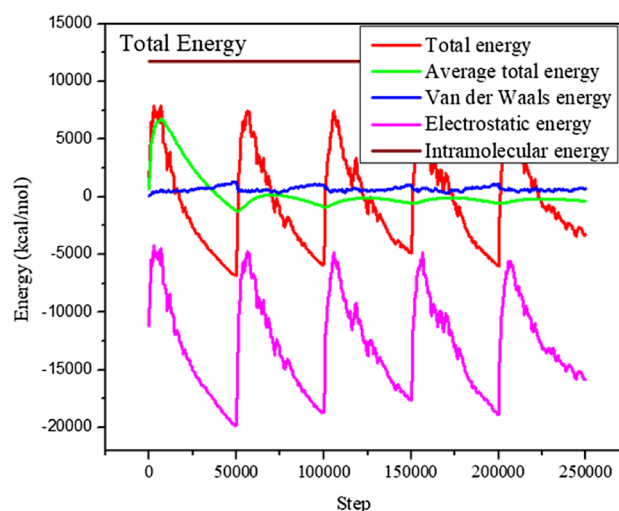**Fig. 13** Energy profile diagrams for the equilibrium adsorption configurations for Al (110)/DGEBAAA + $600H_2O$ + $100Na^+$ and $100Cl^-$ ions system

the system. The resulting equilibrium adsorption configurations for Al (111)-DGEBAAA + $600H_2O$ + $100Na^+$ and $100Cl^-$ ions system are shown in Fig. 14 as a representative specimen of the modeled adsorption system.

The monomer DGEBAAA coating molecules were adsorbed onto Al (111) clean surface in a flat mode, ensuring the maximum interactions of the heteroatoms (Aminoamide) with the metallic surface.

The parameters presented in Table 4 include the total energy (E_{Total}) of the substrate/adsorbate system. The E_{Total} is defined as the sum of the adsorption energy (E_{Ads}) and the internal energy of the sorbate. Furthermore, the E_{Ads} of the DGEBAAA repeat unit on the surface of the Al ($1\bar{1}1$) in the presence of the water molecule.

The tabulated data demonstrate that the predicted adsorption energies for all species are negative, quantitatively implying the adsorption capability of DGEBAAA polymer chain on the Al (111) substrate.

3.7 Anticorrosion Properties of the DGEBAAA Polymer

On the basis of combined computational modeling and experimental results, a simple coating mechanism is proposed for Al (111) surface coated with DGEBA-polyaminoamide. The presence of N and O atoms and aromatic rings allows the DGEBAAA polymer to exhibit a strong interaction with the Al (111) surface. As the observed outcome of the present investigation, DGEBAAA polymer is mainly chemically adsorbed. A proposed mechanism showing the interaction sites between of DGEBAAA polymer and the Al (111) surface is shown in Fig. 15.
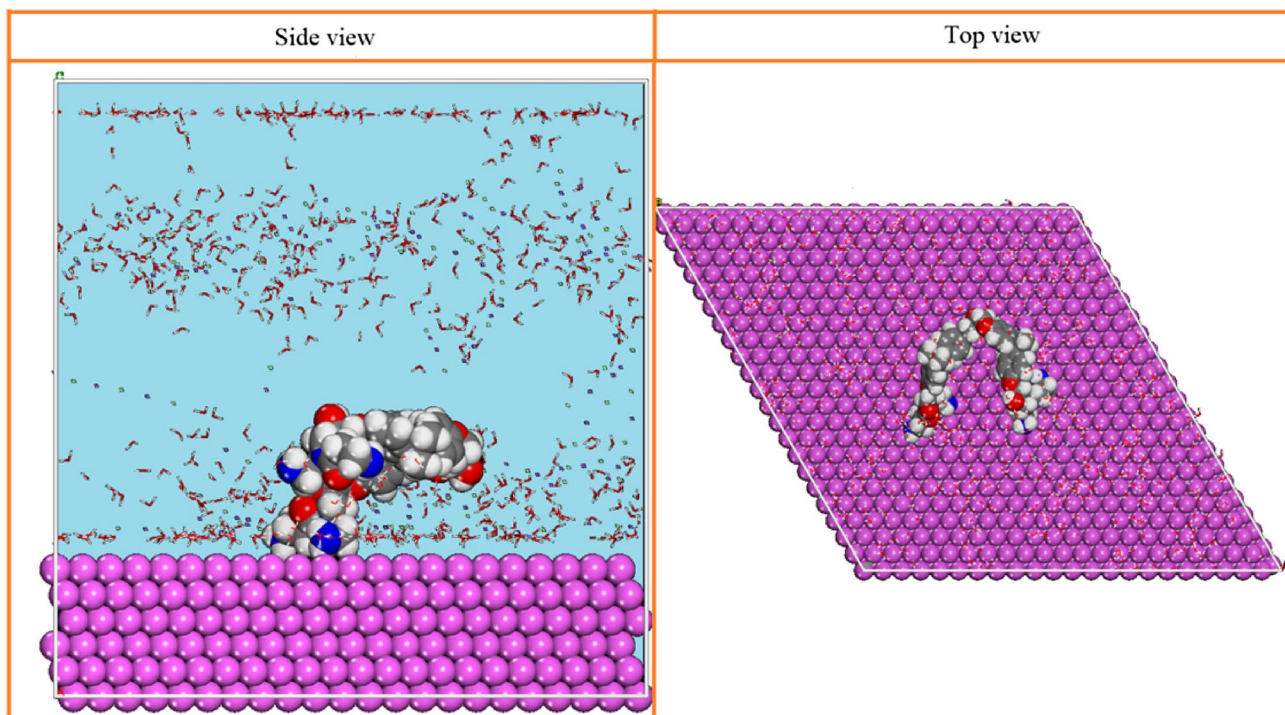

Fig. 12 Adsorption energy distributions for Al (110)/DGEBAAA + $600H_2O$ + $100Na^+$ and $100Cl^-$ ions system using adsorption locator model

Fig. 14 Top and side views of the equilibrium adsorption configurations of the monomer DGEBAAA on Al (111) surface obtained using Monte Carlo simulations

Table 4 Outputs and descriptors calculated by the Monte Carlo (MC) simulation for the adsorption of monomer DGEBAAA on Al (111) surface (all values in Kcal mol^{-1})

Structures	Structure	Total energy (10^4)	Adsorption energy (10^4)	Rigid adsorption energy (10^4)	Deformation energy (10^4)	dE_{ad}/dN_i
DGEBAAA	Al (1 1 1)-1	-2.34	-3.51	-2.37	-1.14	-252.061
	Al (1 1 1)-2	-2.31	-3.49	-2.35	-1.14	-267.240
	Al (1 1 1)-3	-2.30	-3.48	-2.34	-1.14	-210.418
	Al (1 1 1)-4	-2.30	-3.48	-2.34	-1.14	-196.077
	Al (1 1 1)-5	-2.30	-3.47	-2.33	-1.14	-217.942
	Al (1 1 1)-6	-2.29	-3.46	-2.32	-1.14	-191.987
	Al (1 1 1)-7	-2.28	-3.46	-2.32	-1.14	-241.778
	Al (1 1 1)-8	-2.28	-3.46	-2.31	-1.14	-200.026
	Al (1 1 1)-9	-2.28	-3.46	-2.31	-1.14	-143.957
	Al (1 1 1)-10	-2.28	-3.45	-2.31	-1.14	-200.300

4 Conclusions

In this study, the polymeric-based epoxy resin coating on DGEBA-polyaminoamide was prepared and evaluated as anticorrosive coating materials for aluminum surface 2024-T3. The polymeric-based epoxy resin has two functionalities (NH and OH) with high affinity for coordination with metals, which makes it superior anticorrosive coating for aluminum. In addition, the presence of the hydrophobic group in the polymer backbone adds advantage in terms of characteristic superiority. The coated 2024-T3 aluminum was subjected to long- and short-term exposures to an electrolyte solution. The electrochemical measurement results showed an excellent performance of the DGEBA-polyaminoamide epoxy resin as an anticorrosive agent. The results indicate that the DGEBA-polyaminoamide exhibited an excellent performance as a physical barrier with a high coating resistance value. The computational results indicate that the DGEBA-aminoamide coating adheres strongly to the aluminum surface with an adsorption energy of -252 kcal/mol.
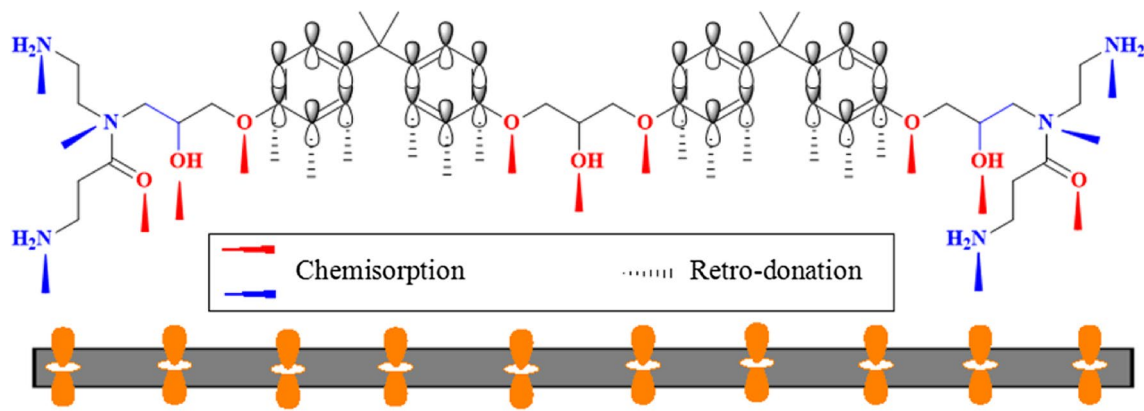
Fig. 15 Pictorial representation of the adsorption of DGEABAAA on Al (111) surface

Compliance with Ethical Standards

Conflicts of interest The authors declare that they have no conflicts to disclose.

References

1. Li Y, Zhang P, Bai P, Wu L, Liu B, Zhao Z (2018) Microstructure and properties of Ti/TiBCN coating on 7075 aluminum alloy by laser cladding. Surf Coat Technol 334:142–149

2. Dagdag O, Essamri A, El Gana L, El Bouchti M, Hamed O, Cherkaoui O et al (2018) Synthesis, characterization and rheological properties of epoxy monomers derived from bifunctional aromatic amines. Polym Bull. https://doi.org/10.1007/s00289-018-2607-4

3. Dagdag O, El Gana L, Hamed O, Erramli H, El Harfi A (2019) Anticorrosive formulation based of the epoxy resin-polyaminoamide containing Zinc phosphate inhibitive pigment applied on sulfo-tartaric anodized AA 7075-T6 in NaCl medium. J Bio-Tribo-Corros 5:25. https://doi.org/10.1007/s40735-019-0218-8

4. Bahlakeh G, Ghaffari M, Saeb MR, Ramezanzadeh B, De Proft F, Terryn H (2016) A close-up of the effect of iron oxide type on the interfacial interaction between epoxy and carbon steel: combined molecular dynamics simulations and quantum mechanics. J Phys Chem C 120(20):11014–11026

5. Salgin B, Özkanat O, Mol JM, Terryn H, Rohwerder M (2013) Role of surface oxide properties on the aluminum/epoxy interfacial bonding. J Phys Chem C 117(9):4480–4487

6. Taheri P, De Wit JHW, Terryn H, Mol JMC (2013) In situ study of buried metal-polymer interfaces exposed to an aqueous solution by an integrated ATR-FTIR and electrochemical impedance spectroscopy system. J Phys Chem C 117(40):20826–20832

7. Bahlakeh G, Hasani-Sadrabadi MM, Jacob KI (2016) Exploring the hydrated microstructure and molecular mobility in blend polyelectrolyte membranes by quantum mechanics and molecular dynamics simulations. RSC Adv 6(42):35517–35526

8. Bahlakeh G, Nikazar M (2012) Molecular dynamics simulation analysis of hydration effects on microstructure and

transport dynamics in sulfonated poly (2, 6-dimethyl-1, 4-phenylene oxide) fuel cell membranes. Int J Hydrog Energy 37(17):12714–12724

9. Hasani-Sadrabadi MM, VanDersarl JJ, Dashtimoghadam E, Bahlakeh G, Majedi FS, Mokarram N et al (2013) A microfluidic approach to synthesizing high-performance microfibers with tunable anhydrous proton conductivity. Lab Chip 13(23):4549–4553

10. Dagdag O, Hamed O, Erramli H, El Harfi A (2018) Anticorrosive performance approach combining an epoxy polyaminoamide-zinc phosphate coatings applied on sulfo-tartaric anodized aluminum alloy 5086. J Bio- Tribo-Corros 4(4):52

11. Dagdag O, El Harfi A, El Gana L, Hlimi Z, Erramli H, Hamed O, Jodeh S (2019) The role of zinc phosphate pigment in the anticorrosion properties of bisphenol a diglycidyl ether-polyaminoamide coating for aluminum alloy AA2024-T3. J Bio- Tribo-Corros 5(1):7

12. Grimme S (2006) Semiempirical GGA-type density functional constructed with a long-range dispersion correction. J Comput Chem 27(15):1787–1799

13. Klamt A, Schüürmann GJGJ (1993) COSMO: a new approach to dielectric screening in solvents with explicit expressions for the screening energy and its gradient. J Chem Soc Perkin Trans 2(5):799–805

14. Dagdag O, El Harfi A, El Gouri M, Safi Z, Jalgham RT, Wazzan N et al (2019) Anticorrosive properties of Hexa (3-methoxy propan-1, 2-diol) cyclotri-phosphazene compound for carbon steel in 3% NaCl medium: gravimetric, electrochemical, DFT and Monte Carlo simulation studies. Heliyon 5(3):e01340

15. Dagdag O, El Harfi A, Cherkaoui O, Safi Z, Wazzan N, Guo L et al (2019) Rheological, electrochemical, surface, DFT and molecular dynamics simulation studies on the anticorrosive properties of new epoxy monomer compound for steel in 1 M HCl solution. RSC Adv 9(8):4454–4462

16. El Aoufir Y, Sebhaoui J, Chaouiki A, Lgaz H, Salghi R, Guenbour A et al (2018) Two novel benzodiazepines as corrosion inhibitors for carbon steel in hydrochloric acid: experimental and computational studies. J Bio- Tribo-Corros 4(4):54

17. Mishra A, Verma C, Srivastava V, Lgaz H, Quraishi MA, Ebenso EE, Chung IM (2018) Chemical, electrochemical and computational studies of newly synthesized novel and environmental friendly heterocyclic compounds as corrosion inhibitors for mild steel in acidic medium. J Bio- Tribo-Corros 4(3):32

18. Berendsen HJ, Postma JV, van Gunsteren WF, DiNola ARHJ, Haak JR (1984) Molecular dynamics with coupling to an external bath. J Chem Phys 81(8):3684–3690

19. Sun H, Jin Z, Yang C, Akkermans RL, Robertson SH, Spenley NA et al (2016) COMPASS II: extended coverage for polymer and drug-like molecule databases. J Mol Model 22(2):47

20. Dagdag O, El Harfi A, Essamri A, El Bachiri A, Hajjaji N, Erramli H et al (2018) Anticorrosive performance of new epoxy-amine coatings based on zinc phosphate tetrahydrate as a non-toxic pigment for carbon steel in NaCl medium. Arab J Sci Eng 43:5977–5987

21. Dagdag O, El Harfi A, Essamri A, El Gouri M, Chraibi S, Assouag M et al (2018) Phosphorous-based epoxy resin composition as an effective anticorrosive coating for steel. Int J Ind Chem 9(3):231–240

22. Dagdag O, El Harfi A, El Gouri M, Touhami ME, Essamri A, Cherkaoui O (2016) Electrochemical impedance spectroscopy (SIE) evaluation of the effect of immersion time of the protective matrix based on a polymer tetra glycidyl of ethylene diani-line (TGEDA) on carbon steel in 3% NaCl. Int J ChemTech Res 9(04):390–399

23. Ghasemi-Kahrizsangi A, Shariatpanahi H, Neshati J, Akbar-inezhad E (2015) Corrosion behavior of modified nano carbon black/epoxy coating in accelerated conditions. Appl Surf Sci 331:115–126

24. Wu LK, Zhang JT, Hu JM, Zhang JQ (2012) Improved corrosion performance of electrophoretic coatings by silane addition. Corros Sci 56:58–66

25. Verma C, Quraishi MA, Ebenso EE, Bahadur I (2018) A green and sustainable approach for mild steel acidic corrosion inhibition using leaves extract: experimental and DFT studies. J Bio- Tribo-Corros 4(3):33

26. Rbaa M, Lgaz H, El Kacimi Y, Lakhrissi B, Bentiss F, Zarrouk A (2018) Synthesis, characterization and corrosion inhibition studies of novel 8-hydroxyquinoline derivatives on the acidic corrosion of mild steel: experimental and computational studies. Mater Discov 12:43–54

27. Bahlakeh G, Ramezanzadeh B, Saeb MR, Terryn H, Ghaffari M (2017) Corrosion protection properties and interfacial adhesion mechanism of an epoxy/polyamide coating applied on the steel surface decorated with cerium oxide nanofilm: complementary experimental, molecular dynamics (MD) and first principle quantum mechanics (QM) simulation methods. Appl Surf Sci 419:650–669

28. Hsissou R, Dagdag O, Abbout S, Benhiba F, Berradi M, El Bouchti M et al (2019) Novel derivative epoxy resin TGETET as a corrosion inhibition of E24 carbon steel in 1.0 M HCl solution. Experimental and computational (DFT and MD simulations) methods. J Mol Liq 284:182–192

29. Adam MSS, El-Lateef HMA, Soliman KA (2018) Anionic oxide-vanadium Schiff base amino acid complexes as potent inhibitors and as effective catalysts for sulfides oxidation: experimental studies complemented with quantum chemical calculations. J Mol Liq 250:307–322

30. Ji YX, Wang FH, Duan LC, Zhang F, Gong XD (2013) Effect of temperature on the adsorption of sulfanilamide onto aluminum oxide and its molecular dynamics simulations. Appl Surf Sci 285:403–408